

## Plasmonic absorption in textured silver back reflectors of thin film solar cells

F.-J. Haug,<sup>a)</sup> T. Söderström, O. Cubero, V. Terrazzoni-Daudrix, and C. Ballif

*Institute of Microtechnology, University of Neuchâtel, Rue A.-L. Breguet 2, Neuchâtel CH-2000, Switzerland*

(Received 29 February 2008; accepted 27 July 2008; published online 24 September 2008)

We study the influence of different textures and dielectric environments on the excitation of surface plasmon resonances on silver because textured metallic films often serve as back contacts of silicon thin film solar cells. For coupling between light and the surface plasmon excitation we use a periodic sinusoidal structure that enables us to sample the dispersion relation at well defined conditions with a simple spectral reflection measurement. We use three layer samples of amorphous silicon/ZnO/silver to mimic the behavior of the back contact in a thin film silicon solar cell; the measurements suggest that losses due to plasmon excitation can very well extend in the spectral region where optimum reflectance is desired. An appropriate thickness of ZnO is able to reduce absorption losses. Our findings on periodic structures are also found useful to explain the behavior of surface plasmon excitation on randomly textured ZnO/Ag reflector layers. © 2008 American Institute of Physics. [DOI: 10.1063/1.2981194]

### I. INTRODUCTION

Surface plasmon polaritons (SPPs) are propagating waves of the surface charge density at the interface of a metal with a dielectric. Their first observation by Ritchie<sup>1</sup> immediately triggered a vast interest in the subject. On flat metallic surfaces the direct interaction between the plasmon and incident light is prohibited. Coupling to radiation becomes possible either by surface modulations,<sup>2-4</sup> by using the evanescent light mode of attenuated total reflection (Otto<sup>5</sup> configuration), or by exciting the through thin metallic films on a prism surface (Kretschmann<sup>6</sup> configuration). The early developments are well covered by the books of Raether,<sup>7,8</sup> whereas recent results are reviewed in several articles, e.g., Refs. 9–12.

Plasma oscillations can also be excited in metallic nanoparticles. They are often called localized plasmons because they correspond to collective oscillations of the conduction electrons within the particle rather than traveling waves on the surface. Enhanced field intensities in the vicinity of localized plasmons have been used for enhancing the photocurrent in organic semiconductor solar cells, where poor charge carrier mobility necessitates very thin absorber structures.<sup>13-15</sup> Recently, silver nanoparticles were also reported to improve the photocurrent thin film silicon solar cells.<sup>16,17</sup>

In general the excitation of SPPs is undesired for solar cell operation because the absorption in any of the supporting films is unlikely to create electron hole pairs and is therefore considered a potential loss mechanism. Their excitation is a particular problem for thin film silicon solar cells for two reasons. First, the absorption of light into SPPs in the metallic back contact necessarily interferes with the aim of reflecting as many photons as possible back into the absorber layer. Second, in silicon thin film solar cells the interfaces includ-

ing the metal back contact are intentionally textured in order to enhance the diffuse scattering of light. However, exactly this texture will also promote the excitation of SPPs. In general, it is difficult to exploit arbitrary structures for enhanced light scattering and at the same time avoid reflection losses due to the excitation of SPPs.<sup>18-20</sup> The situation is different for periodic structures; in principle, the absorption of surface plasmon resonances can be shifted into an uncritical spectral range by choosing the periodicity of the structure. For a given period, the effectiveness of diffraction can still be adopted in a comparatively wide range by the depth and the form of the structure (e.g., sinusoidal, rectangular, blazed, saw tooth, etc.).<sup>21-23</sup> Recently, the authors found excellent light trapping on a two-dimensional grating structure, which yielded a current density of more than 23 mA/cm<sup>2</sup> in a microcrystalline silicon solar cell with an absorber layer thickness of only 1.2  $\mu\text{m}$ .<sup>24</sup>

In this contribution we present experimental observations of surface plasmon excitation in multilayer systems of silver, zinc oxide, and amorphous silicon, which are typically used in thin film silicon solar cells. The investigation does not intend to exhaust the underlying theory; rather, we attempt to explain our findings by considering the relatively simple case of the flat surface where the grating is a perturbation that primarily serves as tool for the controlled excitation of plasmon resonances. This makes our findings also applicable to the much wider class of arbitrary textures of moderate roughness.

### II. EXPERIMENTAL

The gratings studied in this investigation were supplied externally (OVD Kinegram AG). They were fabricated by large area roll-to-roll replication of a grating master into the surface of transparent plastic substrates such as poly(ethylene terephthalate) and poly(ethylene naphthalate). The process is fully compatible with large area requirements of solar cell applications and is applicable not only to gratings but

<sup>a)</sup>Electronic mail: franz-josef.haug@unine.ch.

also to a wide range of arbitrary surface structures. In this study we used an exemplary grating, which consists of a one-dimensional sinusoidal structure with a period of 890 nm and an amplitude of 70 nm (half the peak to valley depth). The textured plastic substrates were covered with sputtered films of silver and zinc oxide without intentional heating of the plastic substrate (Univex 450B, Leybold). The amorphous silicon was fabricated by plasma enhanced chemical vapor deposition at 70 MHz and a substrate temperature of 190 °C from a silane/hydrogen mixture with dilution  $[H_2]/[SiH_4]$  equal to 2. Reflection and transmission spectra for the visible and near IR were recorded with non-polarized light in a spectrometer with integrating sphere (Lambda 900, Perkin Elmer). Measurements in the mid-IR range were carried out with a Fourier transform infrared spectrometer (Nicolet 8700, Thermo). The spectral measurement of the absorption dips slightly limits the resolution compared to an angular scan at fixed wavelength, but it gives access to a wider range of wave vectors in a single measurement.

### III. THEORY

For metals, often the imaginary part of the dielectric function  $\varepsilon''$  is much smaller than the absolute value of the real part  $\varepsilon'$ . In this case, the dispersion relation of a SPP on a flat, semi-infinite metal surface is given by [see, e.g., Ref. 8, Eqs. (2.5) and (2.6)]

$$k'(\omega) = \pm \frac{\omega}{c} \left( \frac{\varepsilon_1 \varepsilon_2'(\omega)}{\varepsilon_1 + \varepsilon_2'(\omega)} \right)^{1/2}, \quad (1)$$

$$k''(\omega) = \frac{\omega}{c} \frac{\varepsilon_2''(\omega)}{2[\varepsilon_2'(\omega)]^2} \left[ \frac{\varepsilon_1 \varepsilon_2'(\omega)}{\varepsilon_1 + \varepsilon_2'(\omega)} \right]^{3/2}. \quad (2)$$

In these equations  $k$  is the wave vector of the plasmon propagation and  $\varepsilon_1$  and  $\varepsilon_2$  are the dielectric functions of air, or a dielectric, and the metal, respectively. The prime and the double prime denote the real and the imaginary parts, respectively. Thus,  $k''$  represents damping in the direction of propagation along the plane of the interface; it should not be mistaken with the penetration depth vertically into the adjacent materials.<sup>10</sup> The dispersion relations are given in the form  $k(\omega)$  because dielectric functions are normally tabulated with respect to the energy; however, in diagrams usually  $\omega(k)$  is plotted versus  $k$ . For our considerations we use published values for silver.<sup>25</sup> Figure 1 shows the two branches of the real part  $k'$  according to Eq. (1) for the case of the flat silver surface in contact with two different dielectric materials.

Excitation of SPPs by incidence from air or vacuum on a flat metal surface is not possible because the dispersion relation (1) does not intersect with that of a photon [ $k(\omega) = \omega/c$ ]. Surface corrugations, in particular gratings, can mediate the coupling, but in many cases it is a good approximation to consider the dispersion relation of the flat surface also in the presence of moderate surface texture. For the case of a periodic structure the photon can pick up or lose momentum in multiples of the reciprocal lattice vector

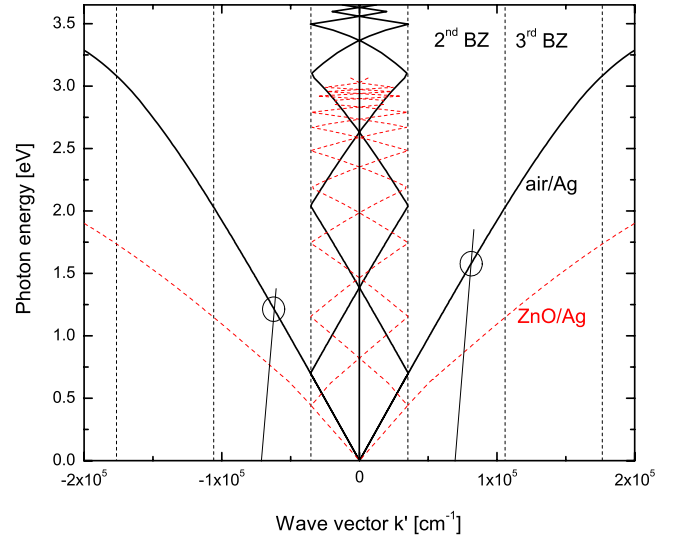


FIG. 1. (Color online) Illustration of extended and reduced Brillouin zone scheme for a grating with a period of  $L=890$  nm. The dashed vertical lines denote the Brillouin zone boundaries. The curves represent the dispersion relations of the silver surface in contact with air (full lines) and with a dielectric (ZnO, dotted lines). For photons incident under  $7^\circ$ , interactions are illustrated at 1.2 and 1.6 eV after shifting left and right by one reciprocal lattice vector  $G=2\pi/L$ , respectively.

$$k' = k_0 \sin \theta + m \cdot \frac{2\pi}{L}. \quad (3)$$

Here the quantity  $k_0$  is a wave vector of the photon in vacuum,  $\theta$  is the angle of incidence with respect to the surface normal,  $L$  is the period of the grating, and  $m$  is an integer. Figure 1 illustrates the definition of Brillouin zones and includes the dispersion relation of flat surface SPPs in reduced zone scheme for a period of 890 nm.

For the description of thin films at least three regions must be considered. The properties of SPPs for this case are conveniently obtained by requiring the denominator of the three layer Fresnel equations to equal zero. For a given energy, this yields an implicit equation for the complex wave vector of the plasmon resonance  $\beta=k'+ik''$  (Refs. 8 and 26)

$$(\varepsilon_2 S_1 + \varepsilon_1 S_2)(\varepsilon_2 S_3 + \varepsilon_3 S_2) - (\varepsilon_2 S_1 - \varepsilon_1 S_2)(\varepsilon_2 S_3 - \varepsilon_3 S_2) \exp\{-2S_2 d\} = 0. \quad (4)$$

Here  $\varepsilon_1$ ,  $\varepsilon_2$ , and  $\varepsilon_3$  represent the dielectric functions of the incident medium, the film with its thickness  $d$ , and the substrate, respectively, and  $S_i^2 = \beta^2 - \varepsilon_i k_0^2$ ,  $k_0$  being again the wave vector of a photon in vacuum.

### IV. RESULTS AND DISCUSSION

We studied the surface plasmon absorption in the periodically textured reflector in three different situations. First, we investigated SPPs on thin silver films where the thickness was varied between 30 and 90 nm. In a second series of experiments we used a three layer system to study the effect of thin ZnO films on the dispersion relation of silver, and we investigated the effect of ZnO films sandwiched between amorphous silicon and silver. Stacks of this third type repre-

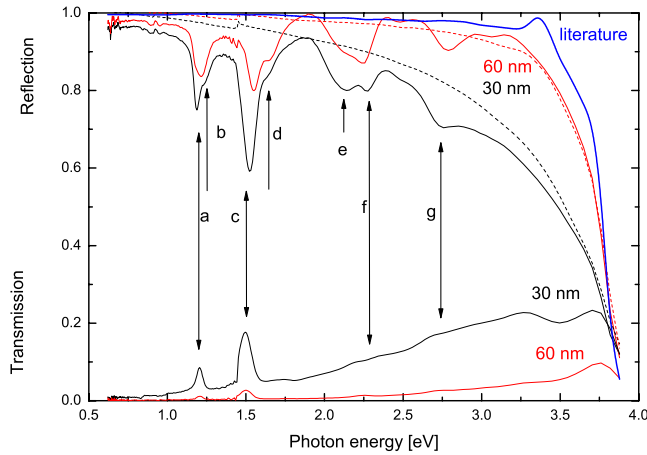


FIG. 2. (Color online) Reflection and transmission measurements of silver films on the grating for silver thicknesses of 30 and 60 nm (full lines) and bulk reflection according to literature. Dashed curves represent the reflection of the respective flat references. Light is incident from the silver side under an angle of  $7^\circ$ .

sent a model for thin film silicon solar cells. Finally, we relate the absorption on randomly structured ZnO/Ag reflectors to our findings on the periodic structure.

### A. Thin silver films on gratings

Figure 2 presents reflection and transmission spectra of two silver films with different thicknesses on the grating. The spectra have been obtained by illuminating from the silver side under an incident angle of  $7^\circ$ . Some ambiguity arises in attributing the origin of the different dips. The doublet at 1.2 eV consists of a low energy part [Fig. 2(a)] whose depth depends on the thickness of the silver layer and a second dip [Fig. 2(b)], which is essentially independent of the silver thickness. We attribute the low energy dip [Fig. 2(a)] to a plasmon excitation at the air/silver interface, which is mediated by one reciprocal wave vector. The transmission measurement in Fig. 2 shows a peak at the same energy and with the same thickness dependence, which means that SPP resonance can radiate into the substrate. For the 30 nm thick film the transmission increases from the 3% background value to more than 8%. The transmission effect is drastically reduced on the 60 nm sample no longer visible on the 90 nm sample (not shown). The depth of the reflection dip also decreases but shows saturation close to the level of the 60 nm sample, suggesting that this is the absorption of the silver surface plasmon under the given conditions. For solar cell applications we prefer a thickness of about 90 nm because of its complete reflection.

The feature [Fig. 2(b)] on the high energy side has been identified with the onset of diffraction into first order ( $-1$  order).<sup>27</sup> There is a dip in reflection because, close to pass-off, the first order beam propagates at grazing angles over the surface and will most probably not reach the integrating sphere. For the amplitude of our grating we estimate that close to onset approximately 8% of the reflected intensity is diffracted into the first order beam. This agrees well with the extent of the observed reflection dip. Note that the intensities

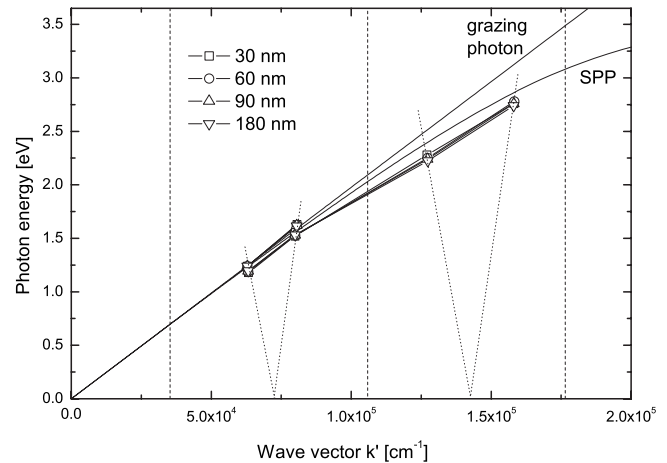


FIG. 3. Positions of the measured reflection dips of the silver layers on the grating (symbols). Full curves show the theoretical dispersion relations for grazing photons and the flat silver surface. For convenience, the diagram has been collapsed into the first quadrant (cf. Fig. 1).

of second and higher order diffraction are much closer to zero at their respective onsets; consequently we do not expect similar dips at shorter wavelengths.

The structure of the doublet (c-d) at 1.6 eV is very similar except that the low energy feature [Fig. 2(c)] shows a deeper dip in reflection and a higher intensity in transmission. For the thinnest film the transmission increases from a background of 5% to almost 18%. The contribution due to diffraction originates from the  $+1$  order.

In the doublet (e-f) between 2.1 and 2.2 eV, the dip [Fig. 2(e)] is again independent of the silver layer thickness, and there is no corresponding feature in transmission. This dip is an artifact of the integrating sphere because it is due to the light of the  $+1$  order beam that leaves through the opening of the reference beam. The artifact [Fig. 2(e)] can be avoided by tilting the sample into a different angle. Thus, dips (f-g) are analogous to Figs. 2(a) and 2(c) but mediated by two reciprocal lattice vectors of the grating. Above 2.5 eV it is no longer possible to resolve individual dips, except for a very weak signature at 3.1 eV. Finally, at 3.8 eV reflection is reduced by bulk excitation in silver.

In the reflection and transmission measurements, we found no signature of SPP excitation at the interface between silver and the polymer substrate. Recently it has been proposed that first order excitations at the interface between layer and substrate are suppressed on gratings with conformal metallic coating.<sup>28</sup> We think that this could explain our observations because our grating is comparatively shallow and we used a nondirectional coating process. Higher order excitations are still expected, but Fig. 2 shows that even on the air/silver interface their intensity is already quite low.

The positions of all dips in terms of energy and wave vector are plotted in Fig. 3. The measured positions roughly follow the trend of the theoretical curve of the flat interface, but the resonances are all shifted toward higher wave vector because the grating represents a perturbation of the ideal flat surface. The effect is well covered in the literature with empiric models,<sup>29</sup> perturbative approaches,<sup>30</sup> and numeric solutions to Maxwell's equations.<sup>31</sup> The detailed presentation in

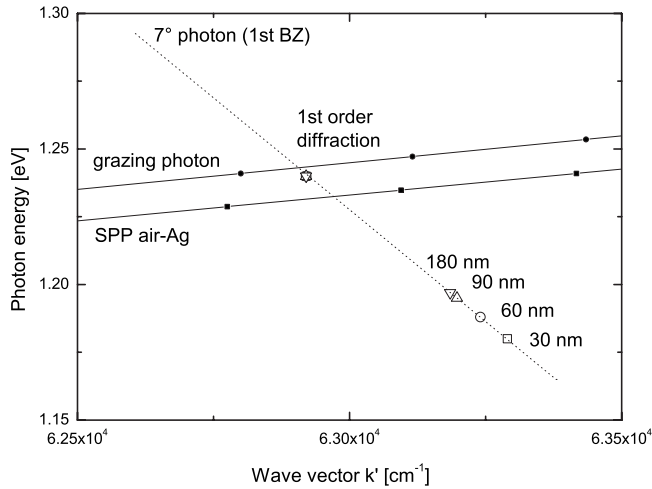


FIG. 4. Details of Fig. 3. The dips related to the onset of first order diffraction are close to the grazing photon line. The measured dips of plasmon resonances are shifted to the right by grating perturbation. Additionally, thickness dispersion of the thin silver films is revealed on this scale.

Fig. 4 actually shows that in the spectroscopic measurement, not only the wave vector is increased, but also the energy is lowered. In fact, in this kind of measurement, the interaction is governed by the geometric constraint of the photon incidence under a certain angle rather than the energy of the excitation. Further, Fig. 4 also reveals the thickness dispersion of the resonance; on thin metal films the surface charges of both interfaces are coupled to each other, and at a given energy, the coupling further increases the wave vectors of the resonances.<sup>26,29,32</sup> The efficiency of the coupling decreases with increasing film thickness. Figure 4 shows that the results on 90 and 180 nm thick films are equivalent. Because the influence of the film thickness is no longer visible, we may regard them like bulk material; their deviation from the flat surface corresponds to what must be considered as perturbation of the grating.

## B. Dielectric layer on metal

In this section we consider a silver reflector with a dielectric coating. Figure 5 presents the measurements of SPP dispersion relations in the ZnO/Ag system for a varied thickness of the ZnO coating. For increasing ZnO thickness the measured branches show a transition from the theoretical curve of the air/Ag interface to that of the ZnO/Ag interface. The calculated dispersion relation using the three layer model assuming a flat, semi-infinite silver substrate coated with 40 nm of ZnO correctly describes the observed trend. Again, the measured curve is located toward higher wave vectors due to the additional influence of the textured surface.

At low energy (long wavelengths), the plasmon resonance at the silver interface is not sensitive to the presence of the dielectric coating. At high energy of about 2 eV a transition between the relations of air/Ag and ZnO/Ag is observed; the ZnO layer of 60 nm acts almost like bulk material, even though at this energy the propagation in the dielectric coating corresponds to less than a fifth of the effective wavelength ( $\lambda_{\text{eff}} = \lambda_0 / \sqrt{\epsilon} \approx 330$  nm). At lower energies Fig. 5 shows

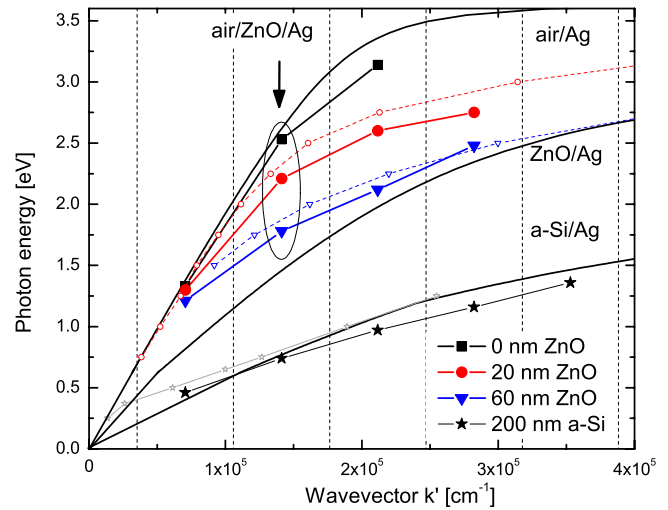


FIG. 5. (Color online) Measurements of SPP absorption dips for silver in contact air (filled squares) and dielectric layers of finite thickness (filled circles: 20 nm ZnO, filled down triangles: 60 nm ZnO, and filled stars: 200 nm *a*-Si layer). All measurements have been performed with perpendicular incidence. Small symbols represent the theoretical dispersion relations for the flat two interface model according to Eq. (4) for 20 nm of ZnO (open circles), 60 nm of ZnO (open down triangles), and 200 nm *a*-Si (open stars).

measurements for the case of 200 nm of amorphous silicon on silver. The figure illustrates that this thickness is sufficient to be considered like bulk material for the energy range above 0.6 eV. However, in this range a dielectric coating is also able to support guided modes<sup>33,34</sup> whose onset is expected as soon as a quarter of the effective wavelength fits into the layer<sup>35</sup> (propagation of the lowest order guided *s*-wave). In the reflection spectra, this results in a wealth of absorption dips; thus, only the unambiguous low energy contributions of plasmon resonances have been plotted in Fig. 5.

## C. Solar cell model

In this section we present measurements on the ZnO/Ag samples with an additional coating of amorphous silicon. This structure very much resembles the application of a dielectric reflector in a thin film silicon solar cell. From Eq. (2) we find that the damping (i.e., absorption losses due to plasmon excitation) scales with the dielectric function of the material in contact with the metal. This suggests the introduction of a low index buffer layer that reduces undesirable plasmon excitations of the *a*-Si/Ag interface. Indeed, in most thin film silicon solar cells with textured silver back reflector, a low index ZnO buffer layer is used,<sup>36,37</sup> which is sometimes also referred to as “detached reflector.”<sup>38</sup>

The dependence of plasmon absorptions on the thickness of a low index buffer layer has been thoroughly treated in the literature, alas for a different reason. Just by replacing the low index layer with an air gap and the silicon film with a prism, we obtain the well-known Otto configuration<sup>39–41</sup> where an air gap of a certain thickness is needed for preventing the prism’s interference with the sample surface. Likewise, for a potential application in the solar cell, we would like to find the required thickness of the buffer (and possibly the ideal buffer material) that prevents the silver surface of the reflector from feeling the presence of the silicon absorber

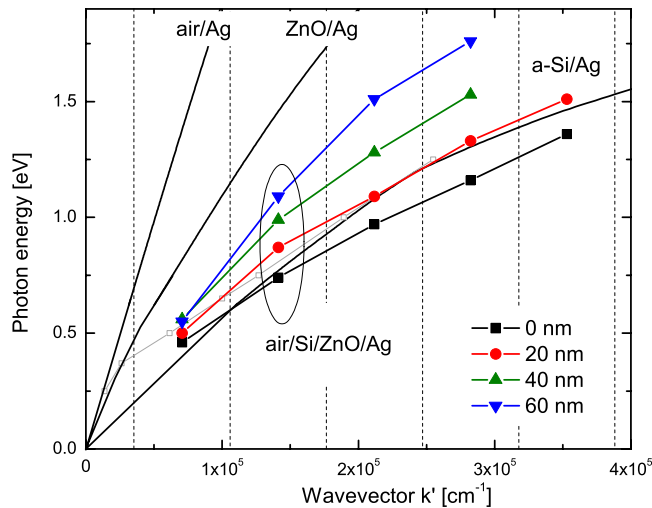


FIG. 6. (Color online) Measurements of SPP absorption dips in *a*-Si/ZnO/Ag stacks show a transition between the *a*-Si/Ag and the ZnO/Ag interface with increasing thickness of the ZnO layer.

layer. Figure 6 shows that a ZnO layer between *a*-Si and silver is indeed capable of shifting the dispersion relation up toward the curve that corresponds to the ZnO/Ag interface.

If the current grating was used for solar cell fabrication, the plasmon absorption at the back contact could be avoided relatively simply. First, for a given absorber material we have to define the energy range where high reflection is required. This would be 1.1 to 1.5 eV for microcrystalline cells and 1.7 to 1.9 eV for amorphous cells. Second, for the case of perpendicular incidence the energies of plasmon absorption can be read directly from the experimentally determined curves in Fig. 6. We find that the structure with a ZnO layer of 60 nm has absorptions at 1.1, 1.5, and 1.8 eV. This particular case would thus be useful for microcrystalline cells (assuming similar refractive index) but only of limited use for amorphous cells. Third, for the given period it still remains to determine the correct depth for achieving the suppression of zero order reflection in the required wavelength range. For the shown example of a sinusoidal grating, this task would be straightforward because the intensities of the different orders are given by Bessel functions.<sup>42</sup>

#### D. Random surface

After this somewhat simplified consideration we conclude the experimental section with the properties of plasmon excitation on random textures. In the absence of a well defined periodicity, we may be able to use the surface correlation length for the definition of a quantity that corresponds to the reciprocal lattice vector of periodic textures. However, we have to keep in mind that a broad range of wave vectors centered on this value will be able to mediate plasmon excitations.<sup>43</sup> Consequently, we expect broad, poorly defined absorption features. A more detailed understanding might require the inclusion of localized phenomena on pointed surface protrusions, where the ideas that have been developed from the case of the flat surface clearly no longer apply.

At high energy where the dispersion relations flatten out, the properties of plasmon excitation are different from the

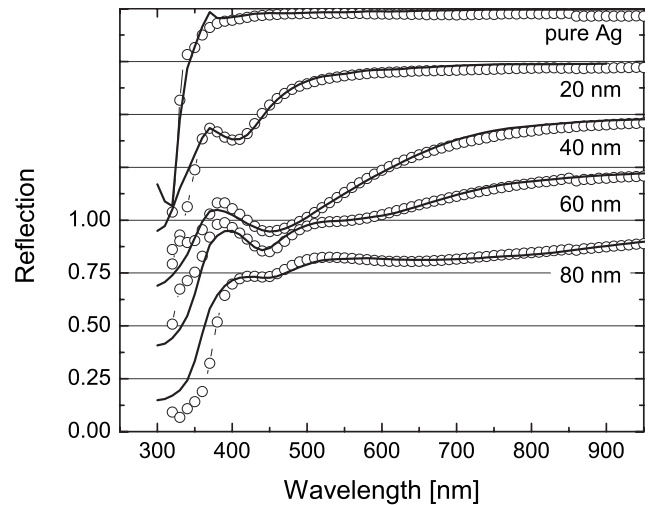


FIG. 7. Reflection measurements of ZnO/Ag on the random structure (open symbols). The ZnO thickness varies between 0 and 80 nm. The vertical scale corresponds to the sample with the thickest ZnO layer. All other curves have been shifted vertically for better visibility. The full curves show fit curves using two Lorentz oscillators.

above considerations; because all wave vectors have the same energy, the energy-momentum conservation is relaxed.<sup>44</sup> Consequently, in this regime plasmon excitation can be mediated by any kind of texture, periodic or arbitrary alike. From Eq. (1) we observe that this situation corresponds to a vanishing denominator (i.e.,  $\epsilon_1 + \epsilon_2 = 0$ ), which should be the case for energies of 3.6, 3.0, and 1.9 eV considering the interfaces of silver with air, ZnO, and *a*-Si, respectively. From our experimental data, we expect slightly lower energies because of perturbation by the surface structure. Surface plasmon absorptions in this regime have previously been reported for randomly textured surfaces. Springer<sup>20</sup> found absorption phenomena at 3.5 and 2.8 eV for the air/silver and the ZnO/silver interfaces, respectively. Similarly, Sainju *et al.*<sup>45</sup> reported ellipsometric investigations of rough ZnO/Ag interfaces where the peak energy of a Lorentzian absorption feature shifts from 3 eV for moderate roughness to 2.75 eV for a rms roughness of 55 nm; the corresponding peak widths vary from 0.4 to 0.7 eV.

We carried out experiments with random surface structures using a replication of the pyramidal surface structure that develops on ZnO grown by low pressure chemical-vapor deposition.<sup>46</sup> Figure 7 shows spectral reflection measurements for ZnO/Ag bilayers on this surface. In addition to the expected bulk absorption in Ag and band gap absorption in ZnO, we observe an additional deep reflection dip that shifts with increasing ZnO thickness from 390 nm (3.2 eV) to 450 nm (2.75 eV). We tentatively assign this feature to the flattened out high energy part of the dispersion relations. From Fig. 5 we expect that this feature will shift toward lower energy with increasing ZnO thickness. Figure 7 shows that a second absorption feature develops at higher wavelengths; on the samples with thin ZnO it is weak shoulder, but for ZnO thickness of 60 and 80 nm it develops into a well defined, broad structure.

Following the procedure of Sainju *et al.*,<sup>45</sup> we modeled the rough interface between silver and ZnO with an interfa-

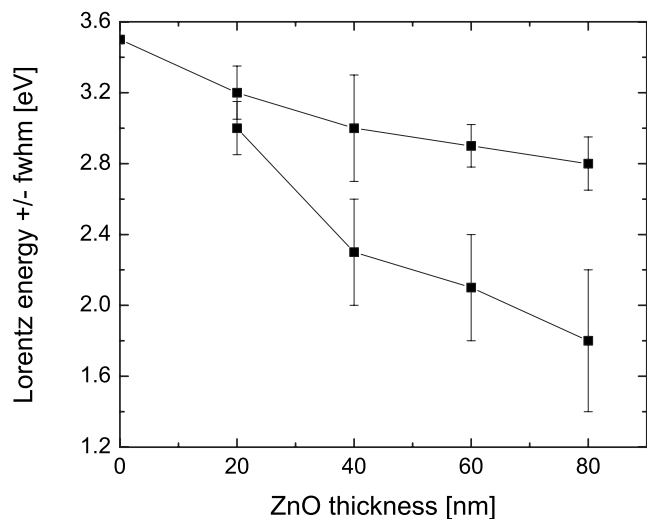


FIG. 8. Energy and full width at half maximum of the Lorentzian oscillators used for fitting the reflection spectra in Fig. 7.

cial layer using the optical simulation software SUNSHINE of the University of Ljubljana.<sup>47</sup> We used a layer thickness of 20 nm that corresponds approximately to the penetration depth into silver at the Ag/ZnO interface.<sup>10</sup> The dielectric function of the interfacial layer was obtained by superimposing the literature data of silver and two Lorentz curves whose position, width, and intensity were varied. The fitted curves are included in Fig. 7. Figure 8 shows the energies and the half widths that were used for the interface layer. We find that the peak energy of the first Lorentz contribution drops from 3.2 to 2.8 eV as the thickness of the ZnO layer is increased from 20 to 80 nm. The second Lorentz curve is difficult to identify for thin ZnO, but the samples with 60 and 80 nm clearly show an absorption feature centered at 2.1 and 1.8 eV, respectively.

Thus, on the ZnO/Ag interface the high energy contribution of texture mediated absorption takes place in an energy range that appears uncritical for solar cells. However, this does not take into account the presence of the silicon absorber layer top of the ZnO. For this situation Fig. 6 clearly reveals that the dispersion relations flatten in an energy range that is indeed very critical. Depending on the thickness of the ZnO buffer, it can be as low as 1.9 eV and even lower if we consider the effect of the perturbation from the flat interface. Further assuming a finite width of the resonances, typically around 0.5 eV, there would be significant absorption of the silver reflector in the spectral range that is relevant for the back reflector of solar cells. Thus, the insertion of a layer with low refractive index is beneficial because it moves the absorption toward higher energies. Indeed, a transparent barrier layer (presumably against diffusion between silicon and the back contact) was found to improve the spectral response of amorphous silicon solar cells at long wavelengths.<sup>37</sup> An optimum barrier layer thickness of 80 nm was found in a systematic study using ZnO on a textured aluminum back contact.<sup>36</sup> While reduced plasmon absorption was often held responsible, we think that our investigation is the first to clearly relate the beneficial effect of this layer to the actual changes in the dispersion relation of the surface plasmon

resonance. It appears that a material with refractive index below that of ZnO could yield still better performance because it would shift the plasmon dispersion relation still higher toward the curve of the air/Ag interface. Recently Buehlmann *et al.*<sup>48</sup> reported the fabrication of phosphorous doped silicon oxide with a refractive index of 1.95 (at 600 nm). Being fully compatible with the *in situ* processing of silicon thin film solar cells, this material could be an interesting candidate for the dielectric buffer layer in textured back reflectors.

Finally, we note that there is a second absorption feature at lower energies. We think that the nature of this absorption is different from the interaction at higher energy that can be mediated by any kind of texture because momentum conservation is relaxed. The absorption at low energy, however, is related to a typical length scale of the surface morphology; in the case of periodicity the result is a narrow absorption that is defined in terms of the reciprocal lattice vector; on the random surface it is a broad feature corresponding to a distribution of length scales around the correlation length.

## V. CONCLUSIONS

We studied the effect of different dielectric environments on the surface plasmon resonance of silver films, which are deposited conformally on a periodically textured substrate. This allows the investigation of plasmon resonances under well defined conditions via grating coupling. By combining a spectral reflectivity measurement with the known periodicity of the grating, we can determine the dispersion relation by sampling of individual points in a wide spectral range. Measurements of the interfaces between air, ZnO, and amorphous silicon in contact to silver are in good agreement with the predictions of a three layer model. For the latter case we find that absorption due to the excitation of texture mediated surface plasmon resonances is likely to occur at energies below 1.9 eV. The corresponding reduction in reflection is detrimental for the operation of a thin film silicon solar cell. In practice often a buffer layer such as ZnO is inserted between silicon and the silver reflector. Our experiments show that the insertion of this buffer layer is capable of shielding the silver surface from feeling the presence of silicon.

## ACKNOWLEDGMENTS

The funding of this work within the European Project “Flexcellence” under Contract No. 019948 is thankfully acknowledged.

<sup>1</sup>R. H. Ritchie, *Phys. Rev.* **106**, 874 (1957).

<sup>2</sup>R. H. Ritchie, E. T. Arakawa, J. J. Cowan, and R. N. Hamm, *Phys. Rev. Lett.* **21**, 1530 (1968).

<sup>3</sup>B. Laks, D. L. Mills, and A. A. Maradudin, *Phys. Rev. B* **23**, 4965 (1981).

<sup>4</sup>N. E. Glass, M. Weber, and D. L. Mills, *Phys. Rev. B* **29**, 6548 (1984).

<sup>5</sup>A. Otto, *Z. Phys.* **216**, 398 (1968).

<sup>6</sup>E. Kretschmann, *Z. Phys.* **241**, 313 (1971).

<sup>7</sup>H. Raether, *Excitation of Plasmons and Interband Transitions by Electrons* (Springer, Berlin, 1980).

<sup>8</sup>H. Raether, *Surface Plasmons* (Springer, Berlin, 1988).

<sup>9</sup>W. Knoll, *Annu. Rev. Phys. Chem.* **49**, 569 (1998).

<sup>10</sup>W. L. Barnes, *J. Opt. A, Pure Appl. Opt.* **8**, S87 (2006).

<sup>11</sup>J. M. Pitarke, V. M. Silkin, E. V. Chulkov, and P. M. Echenique, *Rep. Prog. Phys.* **70**, 1 (2007).

- <sup>12</sup>W. L. Barnes, *Nature (London)* **424**, 824 (2003).
- <sup>13</sup>S. Hayashi, K. Kozaru, and K. Yamamoto, *Solid State Commun.* **79**, 763 (1991).
- <sup>14</sup>M. Westphalen, U. Kreibig, J. Rostalski, H. Lüth, and D. Meissner, *Sol. Energy Mater. Sol. Cells* **61**, 97 (2000).
- <sup>15</sup>B. P. Rand, P. Peumans, and S. R. Forrest, *J. Appl. Phys.* **96**, 7519 (2004).
- <sup>16</sup>E. Moulin, P. Luo, J. Sukmanowski, M. Schulte, F. X. Royer, and H. Stiebig, Proceedings of the 22nd European PVSEC, Milan, 2007 (unpublished), p. 2195.
- <sup>17</sup>E. Moulin, J. Sukmanowski, F. X. Royer, and H. Stiebig, Proceedings of the 21st European PVSEC, Dresden, 2006 (unpublished), p. 1724.
- <sup>18</sup>J. Müller, B. Rech, J. Springer, and M. Vanecek, *Sol. Energy* **77**, 917 (2004).
- <sup>19</sup>J. Springer, A. Poruba, L. Mullerova, M. Vanecek, O. Kluth, and B. Rech, *J. Appl. Phys.* **95**, 1427 (2004).
- <sup>20</sup>J. Springer, B. Rech, W. Reetz, J. Muller, and M. Vanecek, *Sol. Energy Mater. Sol. Cells* **85**, 1 (2005).
- <sup>21</sup>C. Eisele, C. E. Nebel, and M. Stutzmann, *J. Appl. Phys.* **89**, 7722 (2001).
- <sup>22</sup>C. Haase and H. Stiebig, *Prog. Photovoltaics* **14**, 629 (2006).
- <sup>23</sup>C. Haase and H. Stiebig, *Appl. Phys. Lett.* **91**, 061116 (2007).
- <sup>24</sup>F.-J. Haug, T. Söderström, M. Python, V. Terrazzoni-Daudrix, X. Niquire, and C. Ballif, "Development of micromorph tandem solar cells on flexible low cost plastic substrates," *Sol. Energy Mater.* (to be published).
- <sup>25</sup>P. B. Johnson and R. W. Christy, *Phys. Rev. B* **6**, 4370 (1972).
- <sup>26</sup>J. J. Burke, G. I. Stegeman, and T. Tamir, *Phys. Rev. B* **33**, 5186 (1986).
- <sup>27</sup>M. Weber and D. L. Mills, *Phys. Rev. B* **27**, 2698 (1983).
- <sup>28</sup>U. Schröter and D. Heitmann, *Phys. Rev. B* **60**, 4992 (1999).
- <sup>29</sup>T. C. Paulick, *J. Appl. Phys.* **64**, 1384 (1988).
- <sup>30</sup>I. Pockrand and H. Raether, *Opt. Commun.* **18**, 395 (1976).
- <sup>31</sup>J. Chandezon, M. T. Dupuis, G. Cornet, and D. Maystre, *J. Opt. Soc. Am.* **72**, 839 (1982).
- <sup>32</sup>D. Sarid, *Phys. Rev. Lett.* **47**, 1927 (1981).
- <sup>33</sup>D. Hornauer and H. Raether, *Opt. Commun.* **7**, 297 (1973).
- <sup>34</sup>I. Pockrand, *J. Phys. D* **9**, 2423 (1976).
- <sup>35</sup>A. Adams, J. Moreland, P. K. Hansma, and Z. Schlesinger, *Phys. Rev. B* **25**, 3457 (1982).
- <sup>36</sup>C. Kothandaraman, T. Tonon, C. Huang, and A. E. Delahoy, Proceedings of the Symposium on Amorphous Silicon Technology (MRS, Anaheim, 1991), p. 475.
- <sup>37</sup>R. Ross, R. Mohr, J. Fournier, and J. Yang, Proceedings of the IEEE PVSC, New Orleans, 1987 (unpublished), p. 327.
- <sup>38</sup>H. W. Deckman, C. R. Wronski, H. Witzke, and E. Yablonovitch, *Appl. Phys. Lett.* **42**, 968 (1983).
- <sup>39</sup>P. K. Tien, R. Ulrich, and R. J. Martin, *Appl. Phys. Lett.* **14**, 291 (1969).
- <sup>40</sup>L. Wendler and R. Haupt, *Phys. Status Solidi B* **143**, 131 (1987).
- <sup>41</sup>M. Klopfleisch, M. Golz, and U. Trutschel, *Appl. Opt.* **31**, 5017 (1992).
- <sup>42</sup>P. Beckmann and A. Spizzichino, *The Scattering of Electromagnetic Waves from Rough Surfaces* (Artech House, Norwood, MA, 1987).
- <sup>43</sup>V. Celli, A. A. Maradudin, A. M. Marvin, and A. R. McGurn, *J. Opt. Soc. Am. A Opt. Image Sci. Vis* **2**, 2225 (1985).
- <sup>44</sup>E. Kretschmann, T. L. Ferrell, and J. C. Ashley, *Phys. Rev. Lett.* **42**, 1312 (1979).
- <sup>45</sup>D. Sainju, P. J. van den Oever, N. J. Podraza, M. Syed, J. A. Stoke, J. Chen, X. Yang, X. Deng, and R. W. Collins, Proceedings of the Fourth World PVSEC, Hawaii, 2006 (unpublished).
- <sup>46</sup>S. Fay, J. Steinhauser, N. Oliveira, E. Vallat-Sauvain, and C. Ballif, *Thin Solid Films* **515**, 8558 (2007).
- <sup>47</sup>J. Krc, F. Smole, and M. Topic, *Prog. Photovoltaics* **11**, 15 (2003).
- <sup>48</sup>P. Buehlmann, J. Bailat, D. Domine, A. Billet, F. Meillaud, A. Feltrin, and C. Ballif, *Appl. Phys. Lett.* **91**, 143505 (2007).